High-Quality Thin Graphene Films from Fast Electrochemical Exfoliation

Ching-Yuan Su,[†] Ang-Yu Lu,[†,‡] Yanping Xu,[†] Fu-Rong Chen,[‡] Andrei N. Khlobystov,[§] and Lain-Jong Li[†,*]

[†]Research Center for Applied Sciences, Academia Sinica, Taipei 11529, Taiwan, [‡]Department of Engineering and System Science, National Tsing Hua University, 101, Section 2 Kuang Fu Road, Hsinchu 300, Taiwan, and [§]School of Chemistry, The University of Nottingham, University Park, Nottingham, NG7 2RD, U.K.

ABSTRACT Flexible and ultratransparent conductors based on graphene sheets have been considered as one promising candidate for replacing currently used indium tin oxide films that are unlikely to satisfy future needs due to their increasing cost and losses in conductivity on bending. Here we demonstrate a simple and fast electrochemical method to exfoliate graphite into thin graphene sheets, mainly AB-stacked bilayered graphene with a large lateral size (several to several tens of micrometers). The electrical properties of these exfoliated sheets are readily superior to commonly used reduced graphene oxide, which preparation typically requires many steps including oxidation of graphite and high temperature reduction. These graphene sheets dissolve in dimethyl formamide (DMF), and they can self-aggregate at air−DMF interfaces after adding water as an antisolvent due to their strong surface hydrophobicity. Interestingly, the continuous films obtained exhibit ultratransparency (~96% transmittance), and their sheet resistance is <1k Ω/sq after a simple HNO_3 treatment, superior to those based on reduced graphene oxide or graphene sheets by other exfoliation methods. Raman and STM characterizations corroborate that the graphene sheets exfoliated by our electrochemical method preserve the intrinsic structure of graphene.

KEYWORDS: electrochemical exfoliation · graphene · Raman spectroscopy · transparent conductive film · field-effect transistor

Graphene,[1] an atom-thick graphite, has attracted intensive interest due to its two-dimensional and unique physical properties, such as high intrinsic carrier mobility (~200 000 $cm^2/V \cdot s$),[2] excellent mechanical strength, and elasticity and superior thermal conductivity. Modern electronic devices, including touch screens, flexible displays, printable electronics, light emitters, and solar cells, rely on transparent conducting oxides (TCOs), such as indium tin oxide (ITO) and ZnO/Al(ZnO).[3] However, the brittleness of these films severely limits their applications in flexible devices. In addition, the indium (In) is expected to be depleted in a few years; therefore, it is urgent to seek promising replacements. Graphene is an optically transparent, absorbing only 2.3% of visible light, and highly conducting material. Hence, it is considered as highly promising for replacing ITO materials.

Mechanically exfoliated and epitaxially grown graphene films[4−6] exhibit high quality but are not suitable for large-scale production. Recent works on CVD methods using catalytic metal substrates have shown the capability of growing large-area graphene, greatly encouraging their applications in highly transparent and flexible conducting films,[7−10] although more efforts should be made to lower the production costs, particularly those associated with the high-temperature process and expensive substrates. Chemical exfoliation methods based on the Hummers' method, oxidation of graphite into thin graphene oxide (GO), followed by chemical or thermal reduction, have recently drawn much attention due to the advantages of potentially low-cost and solution-processed fabrication.[11−23] However, the oxidation process severely damages the honeycomb lattices of graphene. Also, the subsequent reduction of GO sheets typically involves high temperature to recover the graphitic structure.[24−31] Moreover, the resistance of the films obtained from reported reduced GO (rGO), ranging from 1k to 70k Ω/sq (<80% transmittance)[27,32−34] or from 31k to19M Ω/sq (at 95% transmittance),[20,27,31,35] is still much higher than that of ITO. Several other exfoliation methods attempting to obtain highly conductive graphene sheets have also been realized: (1) liquid-phase exfoliation of graphite by extended sonication,[36−40] and (2) intercalation and expansion of graphite with volatile agents.[41−45] However, the size of graphene sheets obtained by liquid-phase exfoliation or intercalation of graphite is normally smaller than 1 μm^2. The transparent conducting (TC) film made by such small sheets exhibits transparency from 83 to 90% and resistance from 8000 to 5000 Ω/sq.[36,38,41] The high resistance of these TC films is caused by the damage during exfoliation and large amounts of intersheet junctions. Here we demonstrate a novel one-step approach of

* Address correspondence to lanceli@gate.sinica.edu.tw.

Received for review January 3, 2011 and accepted February 2, 2011.

Published online February 10, 2011
10.1021/nn200025p

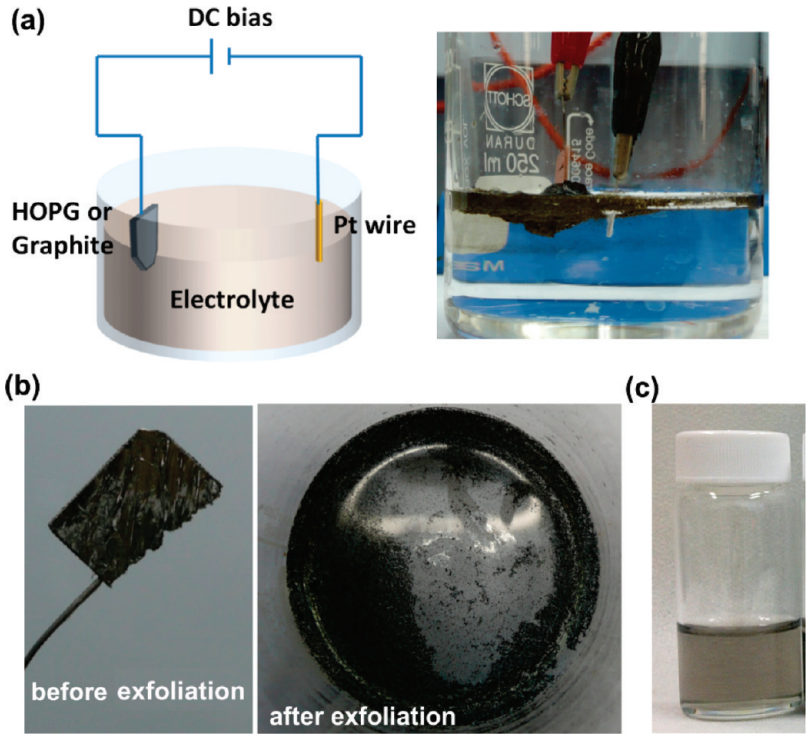

Figure 1. (a) Schematic illustration and photo for electrochemical exfoliation of graphite. (b) Photos of the graphite flakes before and after electrochemical exfoliation. (c) Photo of the dispersed graphene sheets in a DMF solution.

obtaining high-quality graphene thin sheets by electrochemical exfoliation of graphite. The lateral size of the exfoliated graphene sheets ranges from several up to 30 μm, which significantly reduces the number of intersheet junctions for making percolative TC films. The TC film made by these exfoliated graphene sheets exhibits excellent conductivity (sheet resistance is 210 ohm/sq at 96% transparency). Moreover, the effective field-effect mobility extracted from the single-sheet device is readily up to 17 $cm^2/V \cdot s$.

RESULTS AND DISCUSSION

In the past, expandable graphite was prepared by the chemical intercalation of formic acid or sulfuric acid followed by fast heating, where the graphite was violently expanded by gaseous species released from the intercalant (*i.e.*, SO_2).[46,47] However, the majority of the exfoliated graphene flakes was still relatively thick. In this study, we performed the electrochemical exfoliation of graphite in sulfuric acid to obtain high-quality and large-area graphene thin sheets. Figure 1a schematically illustrates our experimental setup, where natural graphite flake (NGF) or highly oriented pyrolytic graphite was employed as an electrode and source of graphene for electrochemical exfoliation. A Pt wire was chosen as a grounded electrode. Many different electrolytes for the electrochemical exfoliation, including HBr, HCl, HNO_3, and H_2SO_4, have been examined, and only the electrolytes containing H_2SO_4 exhibit ideal exfoliation efficiency (see Supporting Information Table S1 for details). When H_2SO_4 solution (4.8 g of 98% H_2SO_4 diluted in 100 mL of deionized (DI) water) was used as an electrolyte, the static bias of +1 V was first applied to the graphite for 5−10 min, followed by ramping the bias to +10 V for another 1 min. The initial low bias helps to wet the sample and likely causes gentle intercalation of SO_4^{2-} ions to the grain boundary of graphite.[46,47] Before applying a high bias of +10 V, the graphite still remained as a single piece. Once the high bias was applied, the graphite was quickly dissociated into small pieces and spread in the solution surface, as shown in Figure 1b. These exfoliated graphene sheets and related products were collected using filtration and redispersed in dimethylformamide (DMF) solution (see Experimental Section for details). Figure 1c shows the photo of the dispersed graphene sheets in DMF solution. We notice that the electrochemical exfoliation of graphene using H_2SO_4 solution is very efficient as the whole exfoliation process can be finished in a few minutes (see Supporting Information video clip 1), but it generally produces thin sheets with high defect level (see Supporting Information Figure S1 for STM, Raman, and ATR-FTIR results) due to the fact that the H_2SO_4 itself also results in strong oxidation of graphite. To reduce the oxidation by H_2SO_4, KOH was added to the H_2SO_4 solution to lower the acidity of the electrolyte solution (2.4 g of 98% H_2SO_4 in 100 mL of DI water, and added with 11 mL of 30% KOH solution to make its pH value around 1.2). Meanwhile, the exfoliation conditions have also been further optimized: The low bias of +2.5 V was applied for 1 min, and then high voltages

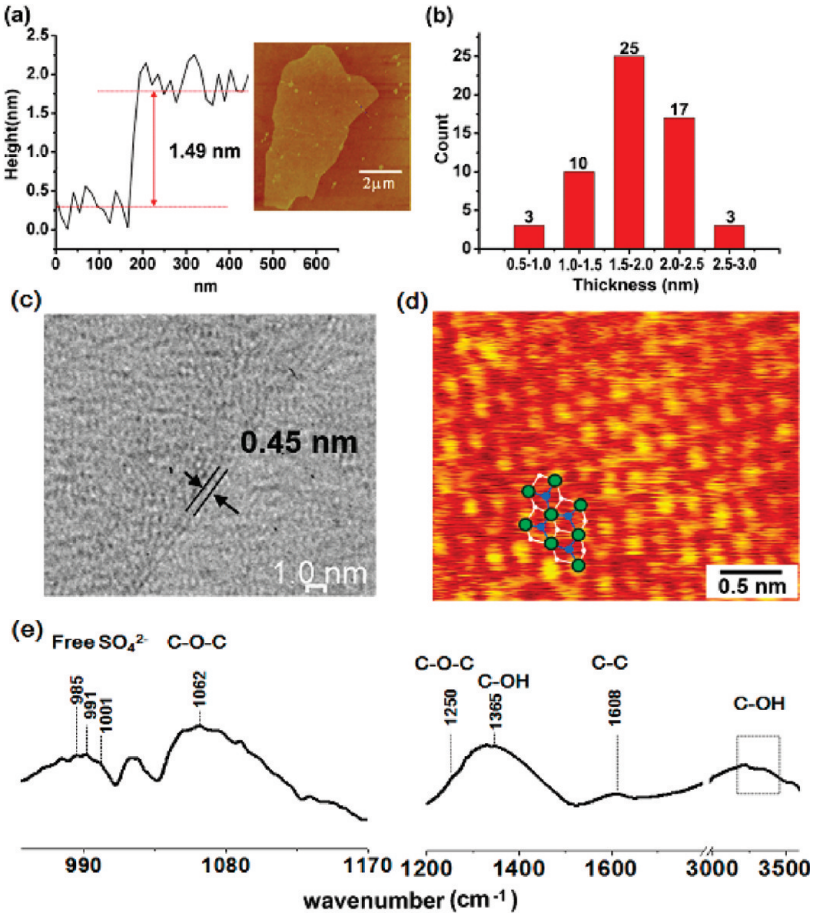

Figure 2. (a) Typical AFM image for an electrochemically exfoliated graphene thin sheet cast on a SiO_2 substrate. (b) Statistical thickness analysis for the graphene sheet ensemble (randomly selected 58 sheets were measured by AFM). (c) Typical TEM image for an exfoliated bilayered graphene. (d) Corresponding STM image of a bilayered graphene, where hexagons indicate the atom configuration of the two layers. (e) ATR-FTIR spectrum acquired from the graphene sheet ensemble.

were applied (alternating between +10 and −10 V) until one obtained desired amounts of exfoliated sheets (see Supporting Information for the video clip 2 showing the electrochemical exfoliation process). The subsequent results and discussions were all based on the exfoliated graphene sheets using this optimized method. Note that the +10 V activated the exfoliation and oxidized the graphene sheets. The produced functional groups are reduced when the bias is switched to −10 V. In the Supporting Information Table S1, we summarize the electrolytes and exfoliation conditions which have been tested. The effects of working voltage and pH dependence on the products are also concluded.

Figure 2a shows a typical AFM image for an electrochemically exfoliated graphene thin sheet (~1.5 nm) drop-cast on a SiO_2 substrate. In Figure 2b, the statistical thickness analysis for the graphene sheet ensemble shows that all of the graphene sheets had a thickness lower than 3 nm and more than 65% of the sheets were thinner than 2 nm. The lateral size of these electrochemically exfoliated graphene sheets ranges from 1 to 40 μm (see Supporting Information Figure S2 for details), significantly larger than those exfoliated in liquid phases with extended sonication.[36−41] It is noted that the total yield of the graphene thin sheets is ~5 to 8 wt %. Figure 2c shows the TEM image typically seen for exfoliated graphene sheet. Our TEM observation reveals that the layer number of these electrochemically exfoliated graphene ranges from 1 to 4 with the most frequently seen graphene as bilayer (see Supporting Information Figure S3 for more TEM analysis). The interlayer distance obtained from high-resolution TEM is about 0.45 nm, which is larger than that of ordinary graphite (0.335 nm). Supporting Information Figure S4 shows more TEM images and statistical analysis for the interlayer distance. Similar phenomenon is also observed in expanded graphite, where the intercalating fluorinated compounds increase the graphene interlayer spacing.[43] Figure 2d shows the STM image from the selected area of this graphene sheet, where the bright lattice pattern marked with circles and spots suggests that the bilayer graphene exhibits A−B stacking (*i.e.*, Bernal stacking).[48] It is worth noting that the STM pattern can be seen in the local areas where top and bottom graphene layers strongly interact with each other. For most of the area, we can only see a hexagonal carbon lattice, as shown in Figure 4a,

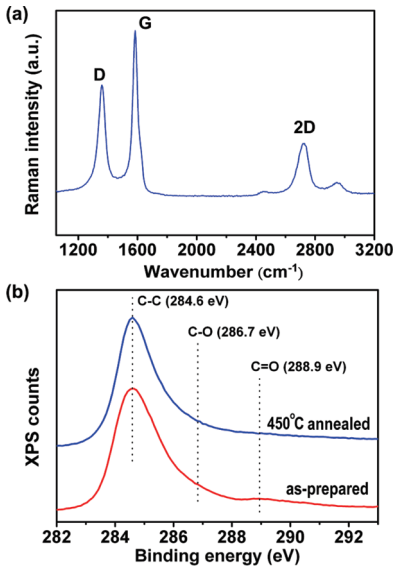

Figure 3. (a) Raman spectrum (excited by 473 nm laser) for the selected graphene with the measured AFM thickness of ~1.6 nm, where D, G, and 2D bands are indicated in the figure. (b) XPS characterizations (C1s binding energy) for the electrochemically exfoliated graphene thin sheets before and after 450 °C thermal annealing.

which could be due to the fact that the interlayer distance is increased and only the top layer graphene can be visualized. The attenuated total reflection Fourier transform infrared (ATR-FTIR) spectrum for the graphene films shown in Figure 2e proves the presence of free (nonbonded) SO_4^{2-} (at 985, 995, and 1001 cm^{-1}), C−O−C (at 1062 and 1250 cm^{-1}), and C−OH (at 1365 cm^{-1} and a broad absorption band at 3000−3500 cm^{-1}).[49,50] The SO_4^{2-} ions are expected to be adsorbed on the surface of exfoliated graphene. The presence of functional groups expands the layer spacing in our graphene sheets, which also explains that the measured AFM thickness for our double-layered graphene (1.5 nm) is slightly larger than the reported value (0.9 to 1.2 nm).[51]

Figure 3a shows the Raman spectrum (excited by 473 nm laser) for the selected graphene with the measured thickness of ~1.6 nm by AFM. It is clearly seen that the graphene sheet exhibits an intense 2D band at around 2720 cm^{-1}. Although the 2D/G ratio (the integrated peak ratio for 2D over G bands) for a bilayered graphene is known to be lower than that for a monolayered graphene,[51−54] the 2D/G for our bilayered graphene is already significantly higher than those for the reduced graphene oxide monolayer. Note that the 2D/G ratio has been shown to be related to the degree of recovery for sp^2 C═C bonds (graphitization) in graphitic structures.[50] Therefore, the quality of the graphene obtained from the electrochemical exfoliation is better than rGO. However, we also notice that a pronounced D band exists in the Raman spectra, which is likely attributed to the unavoidable oxidation by sulfuric acid and the positive electrical potential applied for exfoliation. The presence of the XPS C1s binding energy profile at 286.7 eV (C−O) and 288.9 eV (C═O) for the as-prepared graphene ensemble in Figure 3b proves that there exist small amounts of oxygenated carbon species in the carbon lattice structure. We have also performed 450 °C thermal annealing (30 min in 20% H_2/Ar environment) on the graphene sheets, and XPS shows slight decrease of C−O and C═O signatures. To further access the quality of the exfoliated graphene sheet, Figure 4a displays the typical STM image obtained from a thin graphene sheet (~1.6 nm thick by AFM measurement), where the hexagonally arranged carbon atomic structure can be readily identified even without performing the noise correction to the image, corroborating the good quality of the exfoliated graphene. The fuzzy area in the STM image is attributed to the surface functional groups, such as C−OH as identified in our XPS and ATR-FTIR spectra, on the basal plane of graphene sheet (also see Figure S1b for more severely oxidized graphene exfoliated with H_2SO_4 solution). To evaluate the electrical performance of these graphene sheets, bottom-gate-operated transistors were fabricated by evaporating Au electrodes directly on top of the exfoliated graphene sheets, which were previously deposited on SiO_2/Si substrates. Figure 4b demonstrates the transfer curve (drain current I_d *vs* gate voltage V_g) for the device prepared from an as-prepared single graphene sheet. Inset shows the top view of the device. The field-effect mobility of holes was extracted based on the slope $\Delta I_d/\Delta V_g$ fitted to the linear regime of the transfer curves using the equation $\mu = (L/WC_{ox}V_d)(\Delta I_d/\Delta V_g)$, where L and W are the channel length and width and C_{ox} the gate capacitance.[55] The mobility for the exfoliated graphene sheet ranges from 5.5 to 17 $cm^2/V\cdot s$ in ambient, which is at least an order of magnitude higher than the reported ~0.1−1 $cm^2/V\cdot s$ based on rGO materials.[16,30,31] The statistical analysis for the graphene sheets (with thickness 1.5 to 2 nm), for both as-prepared and after thermal annealing, is shown in Figure 4c. The 450 °C annealing only results in slight improvement in mobility and hence film quality, which agrees with the conclusion drawn from XPS measurement (Figure 3b). We note that the neutrality point (valley point of the transfer curve) for most of our devices is beyond 100 V (the maxima V_g we applied), suggesting that the graphene sheets are heavily p-doped. Thermal annealing removes some of the chemical defects as evidenced by XPS studies (Figure 3b) but does obviously left-shift the neutrality point. We believe that this is due to the presence of impurity charges (negatively charged ions such as SO_4^{2-} or other impurities from chemicals), which causes the effective p-doping of the graphene sheets. The immediate application of these exfoliated large-size graphene sheets is for ultrathin transparent conducting electrodes. For the preparation of electrodes,

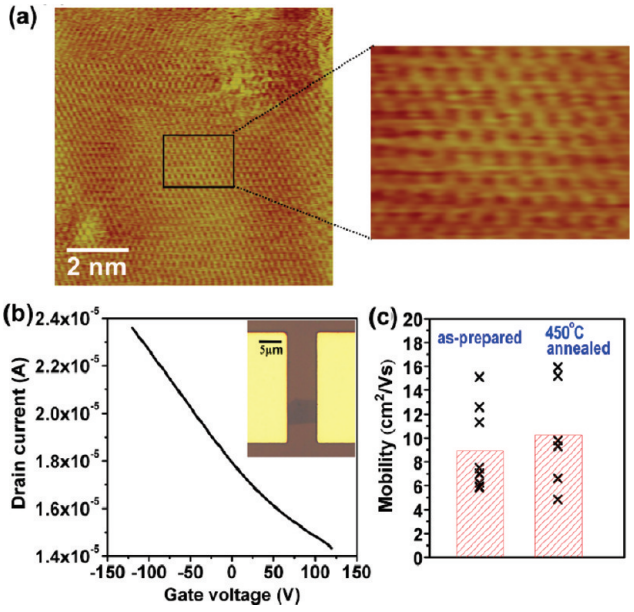

Figure 4. (a) Typical STM image obtained from a thin graphene sheet (~1.5 nm thick), where the hexagonally arranged atomic carbon structure is clearly identified. (b) Transfer curve (drain current I_d *vs* gate voltage V_g) for a device prepared from a single graphene sheet. Inset shows the photograph of the device. (c) Statistical analysis for the graphene sheets (with thickness 1.5 to 2 nm), as-prepared and after thermal annealing. Only graphene sheets with a regular size were selected for the convenience of extracting their effective field-effect mobility.

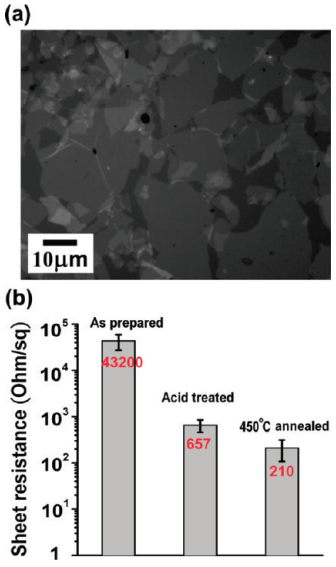

Figure 5. (a) Optical image of the cast thin-conducting electrodes on quartz substrates. (b) Sheet resistance values of as-prepared thin films (with 96% transmittance) and those after acid treatment and after thermal annealing.

a graphene solution with the concentration of 0.085 mg/mL in DMF was dropped (~500 μL) on the substrate, followed by adding small amounts (<200 μL) of water until the very thin graphene aggregation can be visualized at the air−DMF interface (see Experimental Section for details). The sample was then dried in air. Figure 5a shows the optical microscopic image for the thin film formed on a quartz substrate (also see Supporting Information Figure S5 for photos at different length scales). With the careful control for the film formulation process, the exfoliated thin sheets nicely aggregate to form a percolative thin film, in which there are fewer intersheet junctions due to the large size of our sheets. It is therefore beneficial for electrical conduction. Figure 5b shows the sheet resistance values for the thin films (with ~96% transmittance) measured using a four-point-probe system. The sheet resistance for the as-prepared sample is 43200 Ω/sq, and it is largely reduced to ~660 Ω/sq after simple treatment in a 69% of HNO_3 solution (see Experimental Section). This can be simply explained by the hole carrier density increase caused by neutralizing the electron doping from the solvent DMF[56] and also the hole doping by HNO_3 itself. The sheet resistance can be further lowered to ~210 Ω/sq after 450 °C thermal annealing while maintaining its ultrahigh transmittance. We also observed that the film thickness can be adjusted by controlling the poor solvent/solvent (water/DMF) volume ratio used in the segregation process (see Supporting Information Figure S6a). Moreover, the thin films can be transferred onto a flexible and transparent substrate by a roll-to-roll process (see Figure S7 for details). Such low-resistance and high-transparency characteristics likely make these thin films promising for replacing currently used high-cost ITO electrodes in the future.

CONCLUSIONS

In conclusion, a one-step method of obtaining high-quality graphene sheets is demonstrated by electrochemical exfoliation of graphite. The exfoliated graphene sheets exhibit lateral size up to 30 μm.

Most (>60%) of the obtained sheets are bilayered graphene with A−B stacking. The field-effect mobility is up to 17 $cm^2/V \cdot s$, and the TC film made by self-assembled graphene sheets exhibits excellent conductivity (sheet resistance is ~210 ohm/sq at 96% transparency). This work provides an efficient approach to obtain high-quality, cost-effective, and scalable production of "graphene ink", which may pave a way toward future applications in flexible electronics.

EXPERIMENTAL SECTION

Electrochemical Exfoliation of Graphene from Graphite. Natural graphite flakes (NGF) (average size ~5−20 mm from NGS, Germany) or highly oriented pyrolytic graphite (HOPG; 1.5 cm × 1.5 cm × 0.3 mm) was employed as an electrode and source of graphene for electrochemical exfoliation. The graphite flake was adhered to a tungsten wire by a silver pad and then was inserted as anode into the ionic solution. Note that the only graphite was immersed into the solution. A grounded Pt wire was placed parallel to the graphite flake with a separation of 5 cm. The ionic solution was prepared by taking 4.8 g of sulfuric acid (Sigma-Aldrich; 98%) and diluted in 100 mL of DI water. The electrochemical exfoliation process was carried out by applying DC bias on graphite electrode (from −10 to +10 V). To prepare the graphene sheet suspension, the exfoliated graphene sheets were collected with a 100 nm porous filter and washed with DI water by vacuum filtration. After drying, they were dispersed in DMF solution by gentle water-bath sonication for 5 min. To remove unwanted large graphite particles produced in the exfoliation, the suspension was subjected to centrifugation at 2500 rpm. The centrifuged suspension can then be used for further characterizations and film preparation. All of these electrochemical exfoliation experiments were performed at room temperature (25 ± 3 °C).

Characterizations. The AFM images were performed in a Veeco Dimension-Icon system. Raman spectra were collected in a NT-MDT confocal Raman microscopic system (laser wavelength 473 nm and laser spot-size is ~0.5 μm). The Si peak at 520 cm^{-1} was used as reference for wavenumber calibration. STM analysis was carried out on a Veeco STM base in ambient condition. The UV−vis−NIR transmittance spectra were obtained using a Dynamica PR-10 spectrophotometer. XPS measurements were carried out by a Ulvac-PHI 1600 spectrometer with monochromatic Al Kα X-ray radiation (1486.6 eV). The ATR-IR spectra were collected in Perkin-Elmer IR spectrometer. Conductivity measurements of graphene-assembled film were carried out on a Napson RT-70 using a four-point-probe head with a pin distance of about 1 mm. The nanostructure of exfoliated graphene sheets was investigated in a JEOL-2010F TEM with accelerating voltage of 200 keV.

Fabrication of Field-Effect Transistor Devices. The exfoliated graphene sheets were deposited onto the silicon substrates with a 300 nm silicon oxide layer by the dip-coating method, followed by a baking at 190 °C to remove solvent. The field-effect transistor device was fabricated by evaporating Au electrodes (30 nm thick) directly on top of the selected, regularly shaped graphene sheets using a copper grid (200 mesh, 20 μm spacing) as a hardmask. The typically obtained channel length between source and drain electrodes was around 20 μm. The electrical measurements were performed in ambient conditions using a Keithley semiconductor parameter analyzer, model 4200-SCS.

Preparation of Thin-Film Electrodes. For preparing electrodes, quartz or glass substrates were first cleaned with a Piranha solution to remove undesired impurities and to make the surface hydrophilic. The graphene solution with the concentration of 0.085 mg/mL in DMF was dropped (~500 μL) onto the cleaned substrate, followed by adding a drop (100−600 μL) of deionized (DI) water. The thin graphene film was then self-aggregated at the solution surface. After that, the substrates were heated on a hot plate at 190 °C for 30 min to evaporate the residual DMF. To treat the thin-film electrode with HNO_3, the as-prepared samples were dipped in a 69% of HNO_3 solution at 80 °C for 1 h. For the thermal annealing process, the samples were loaded into a quartz tube in a furnace, where a mixture gas of H_2/Ar (20 sccm/80 sccm) was directed into the quartz tube at 450 °C for 30 min (pressure fixed at 500 Torr).

Acknowledgment. This research was supported by Research Center for Applied Science, Academia Sinica (Nano program), and Natinoal Science Council, Taiwan (NSC-99-2112-M-001-021-MY3 and 99-2738-M-001-001).

Supporting Information Available: Raman, STM, TEM, AFM, results, and video clips (the electrochemical exfoliation process) are available. This material is available free of charge *via* the Internet at http://pubs.acs.org.

REFERENCES AND NOTES

1. Novoselov, K. S.; Geim, A. K.; Morozov, S. V.; Jiang, D.; Zhang, Y.; Dubonos, S. V.; Grigorieva, I. V.; Firsov, A. A. Electric Field Effect in Atomically Thin Carbon Films. *Science* **2004,** *306*, 666–669.
2. Bolotin, K. I.; Sikes, K. J.; Jiang, Z.; Klima, M.; Fudenberg, G.; Hone, J.; Kim, P.; Stormer, H. L. Ultrahigh Electron Mobility in Suspended Graphene. *Solid State Commun.* **2008,** *146*, 351–355.
3. Gordon, R. G. Criteria for Choosing Transparent Conductors. *MRS Bull.* **2000,** *25*, 52.
4. Sutter, P. W.; Flege, J.-I.; Sutter, E. A. Epitaxial Graphene on Ruthenium. *Nat. Mater.* **2008,** *7*, 406–411.
5. Liang, X.; Fu, Z.; Chou, S. Y. Graphene Transistors Fabricated *via* Transfer-Printing in Device Active-Areas on Large Wafer. *Nano Lett.* **2007,** *7*, 3840–3844.
6. Berger, C.; Song, Z.; Li, X.; Wu, X.; Brown, N.; Naud, C.; Mayou, D.; Li, T.; Hass, J.; Marchenkov, A. N.; *et al.*Electronic Confinement and Coherence in Patterned Epitaxial Graphene. *Science* **2006,** *312*, 1191–1196.
7. Reina, A.; Jia, X.; Ho, J.; Nezich, D.; Son, H.; Bulovic, V.; Dresselhaus, M. S.; Kong, J. Large Area, Few-Layer Graphene Films on Arbitrary Substrates by Chemical Vapor Deposition. *Nano Lett.* **2009,** *9*, 30–35.
8. Li, X.; Cai, W.; An, J.; Kim, S.; Nah, J.; Yang, D.; Piner, R.; Velamakanni, A.; Jung, I.; Tutuc, E.; *et al.*Large-Area Synthesis of High-Quality and Uniform Graphene Films on Copper Foils. *Science* **2009,** *324*, 1312–1314.
9. Bae, S.; Kim, H. K.; Lee, Y. B.; Xu, X. F.; Park, J. S.; Zheng, Y.; Balakrishnan, J.; Lei, T.; Kim, H. R.; Song, Y.; *et al.*Roll-to-Roll Production of 30-Inch Graphene Films for Transparent Electrodes. *Nat. Nanotechnol.* **2010,** *5*, 574–578.
10. Li, X. S.; Zhu, Y. W.; Cai, W. W.; Borysiak, M.; Han, B. Y.; Chen, D.; Piner, R. D.; Colombo, L.; Ruoff, R. S. Transfer of Large-Area Graphene Films for High-Performance Transparent Conductive Electrodes. *Nano Lett.* **2009,** *9*, 4359–4363.
11. Wassei, J. K.; Kaner, R. B. Graphene, A Promising Transparent Conductor. *Mater. Today* **2010,** *13*, 52–59.
12. Eda, G.; Fanchini, G.; Chhowalla, M. Large-Area Ultrathin Films of Reduced Graphene Oxide as a Transparent and Flexible Electronic Material. *Nat. Nanotechnol.* **2008,** *3*, 270–274.
13. Stankovich, S.; Dikin, D. A.; Piner, R. D.; Kohlhaas, K. A.; Kleinhammes, A.; Jia, Y.; Wu, Y.; Nguyen, S. T.; Ruoff, R. S. Synthesis of Graphene-Based Nanosheets *via* Chemical Reduction of Exfoliated Graphite Oxide. *Carbon* **2007,** *45*, 1558–1565.
14. Park, S.; Ruoff, R. S. Chemical Methods for The Production of Graphenes. *Nat. Nanotechnol.* **2009,** *4*, 217–224.

15. Park, S.; An, J.; Jung, I.; Piner, R. D.; An, S. J.; Li, X.; Velamakanni, A.; Ruoff, R. S. Colloidal Suspensions of Highly Reduced Graphene Oxide in a Wide Variety of Organic Solvents. *Nano Lett.* **2009,** *9*, 1593–1597.
16. Luo, Z.; Lu, Y.; Somers, L. A.; Johnson, A. T. C. High Yield Preparation of Macroscopic Graphene Oxide Membranes. *J. Am. Chem. Soc.* **2009,** *131*, 898–899.
17. Gomez-Navarro, C.; Weitz, R. T.; Bittner, A. M.; Scolari, M.; Mews, A.; Burghard, M.; Kern, K. Electronic Transport Properties of Individual Chemically Reduced Graphene Oxide Sheets. *Nano Lett.* **2009,** *9*, 2206–2206.
18. Williams, G.; Seger, B.; Kamat, P. V. TiO_2-Graphene Nanocomposites UV-Assisted Photocatalytic Reduction of Graphene Oxide. *ACS Nano* **2008,** *2*, 1487–1491.
19. Green, A. A.; Hersam, M. C. Solution Phase Production of Graphene with Controlled Thickness *via* Density Differentiation. *Nano Lett.* **2009,** *9*, 4031–4036.
20. Cote, L. J.; Kim, F.; Huang, J. Langmuir−Blodgett Assembly of Graphite Oxide Single Layers. *J. Am. Chem. Soc.* **2009,** *131*, 1043–1049.
21. Li, D.; Muller, M. B.; Gilje, S.; Kaner, R. B.; Wallace, G. G. Processable Aqueous Dispersions of Graphene Nanosheets. *Nat. Nanotechnol.* **2008,** *3*, 101–105.
22. Gao, W.; Alemany, L. B.; Ci, L.; Ajayan, P. M. New Insights into the Structure and Reduction of Graphite Oxide. *Nat. Chem.* **2009,** *1*, 403–408.
23. Chen, C. M.; Yang, Q. H.; Yang, Y. G.; Lv, W.; Wen, Y. F.; Hou, P. X.; Wang, M. Z.; Cheng, H. M. Self-Assembled Free-Standing Graphite Oxide Membrane. *Adv. Mater.* **2009,** *21*, 3007–3011.
24. Li, X.; Wang, H.; Robinson, J. T.; Sanchez, H.; Diankov, G.; Dai, H. Simultaneous Nitrogen Doping and Reduction of Graphene Oxide. *J. Am. Chem. Soc.* **2009,** *131*, 15939–15944.
25. López, V.; Sundaram, R. S.; Gómez-Navarro, C.; Olea, D.; Burghard, M.; Gómez-Herrero, J.; Zamora, F.; Kern, K. Chemical Vapor Deposition Repair of Graphene Oxide: A Route to Highly-Conductive Graphene Monolayers. *Adv. Mater.* **2009,** *21*, 4683–4686.
26. Becerril, H. A.; Mao, J.; Liu, Z.; Stoltenberg, R. M.; Bao, Z.; Chen, Y. Evaluation of Solution-Processed Reduced Graphene Oxide Films as Transparent Conductors. *ACS Nano* **2008,** *2*, 463–470.
27. Wu, J.; Becerril, H. A.; Bao, Z.; Liu, Z.; Chen, Y.; Peumans, P. Organic Solar Cells with Solution-Processed Graphene Transparent Electrodes. *Appl. Phys. Lett.* **2008,** *92*, 263302-1.
28. Wu, X.; Sprinkle, M.; Li, X.; Ming, F.; Berger, C.; de Heer, W. A. Epitaxial-Graphene/Graphene-Oxide Junction: An Essential Step towards Epitaxial Graphene Electronics. *Phys. Rev. Lett.* **2008,** *101*, 026801-1.
29. Stankovich, S.; Piner, R. D.; Chen, X.; Wu, N.; Nguyen, S. T.; Ruoff, R. S. Stable Aqueous Dispersions of Graphitic Nanoplatelets *via* the Reduction of Exfoliated Graphite Oxide in the Presence of Poly(sodium 4-styrenesulfonate). *J. Mater. Chem.* **2006,** *16*, 155–158.
30. Su, C.-Y.; Xu, Y.; Zhang, W.; Zhao, J.; Tang, X.; Tsai, C.-H.; Li, L.-J. Electrical and Spectroscopic Characterizations of Ultra-Large Reduced Graphene Oxide Monolayers. *Chem. Mater.* **2009,** *21*, 5674–5680.
31. Su, C. Y.; Xu, Y.; Zhang, W.; Zhao, J.; Liu, A.; Tang, X.; Tsai, C.-H.; Huang, Y.; Li, L. J. Highly Efficient Restoration of Graphitic Structure in Graphene Oxide Using Alcohol Vapors. *ACS Nano* **2010,** *4*, 5285–5292.
32. Wang, X.; Zhi, L.; Müllen, K. Transparent, Conductive Graphene Electrodes for Dye-Sensitized Solar Cells. *Nano Lett.* **2008,** *8*, 323–327.
33. Becerril, H. A.; Mao, J.; Liu, Z.; Stoltenberg, R. M.; Bao, Z.; Chen, Y. Evaluation of Solution-Processed Reduced Graphene Oxide Films as Transparent Conductors. *ACS Nano* **2008,** *2*, 463–470.
34. Eda, G.; Lin, Y. Y.; Miller, S.; Chen, C.-W.; Su, W.-F.; Chhowalla, M. Transparent and Conducting Electrodes for Organic Electronics from Reduced Graphene Oxide. *Appl. Phys. Lett.* **2008,** *92*, 233305.
35. Zhu, Y. W.; Cai, W. W.; Piner, R. D.; Velamakanni, A.; Ruoff, R. S. Transparent Self-Assembled Films of Reduced Graphene Oxide Platelets. *Appl. Phys. Lett.* **2009,** *95*, 103104.
36. Hernandez, Y.; Nicolosi, V.; Lotya, M.; Blighe, F. M.; Sun, Z.; De, S.; McGovern, I. T.; Holland, B.; Byrne, M.; Gun'Ko, Y. K.; *et al.*High-Yield Production of Graphene by Liquid-Phase Exfoliation of Graphite. *Nat. Nanotechnol.* **2008,** *3*, 563–568.
37. Blake, P.; Brimicombe, P. D.; Nair, R. R.; Booth, T. J.; Jiang, D.; Schedin, F.; Ponomarenko, L. A.; Morozov, S. V.; Gleeson, H. F.; Hill, E. W.; *et al.*Graphene-Based Liquid Crystal Device. *Nano Lett.* **2008,** *8*, 1704–1708.
38. De, S.; King, P. J.; Lotya, M.; O'Neill, A.; Doherty, E. M.; Hernandez, Y.; Duesberg, G. S.; Coleman., J. N. Flexible, Transparent, Conducting Films of Randomly Stacked Graphene from Surfactant-Stabilized, Oxide-Free Graphene Dispersions. *Small* **2010,** *6*, 458–464.
39. Biswas, S.; Drzal, L. T. A Novel Approach To Create a Highly Ordered Monolayer Film of Graphene Nanosheets at the Liquid−Liquid Interface. *Nano Lett.* **2009,** *9*, 167–172.
40. Gu, W. T.; Zhang, W.; Li, X. M.; Zhu, H. W.; Wei, J. Q.; Li, Z.; Shu, Q. K.; Wang, C.; Wang, K. L.; Shen, W. C.; *et al.*Graphene Sheets from Worm-like Exfoliated Graphite. *J. Mater. Chem.* **2009,** *19*, 3367–3369.
41. Li, X.; Zhang, G.; Bai, X.; Sun, X.; Wang, X.; Wang, E.; Dai, H. Highly Conducting Graphene Sheets and Langmuir−Blodgett Films. *Nat. Nanotechnol.* **2008,** *3*, 538–542.
42. Valles, C.; Drummond, C.; Saadaoui, H.; Furtado, C. A.; He, M.; Roubeau, O.; Ortolani, L.; Monthioux, M.; Penicaud, A. Solutions of Negatively Charged Graphene Sheets and Ribbons. *J. Am. Chem. Soc.* **2008,** *130*, 15802–15804.
43. Lee, J. H.; Shin, D. W.; Makotchenko, V. G.; Nazarov, A. S.; Fedorov, V. E.; Kim, Y. H.; Choi, J. Y.; Kim, J. M.; Yoo, J. B. One-Step Exfoliation Synthesis of Easily Soluble Graphite and Transparent Conducting Graphene Sheets. *Adv. Mater.* **2009,** *21*, 4383–4387.
44. Lu, J.; Yang, J. X.; Wang, J.; Lim, A.; Wang, S.; Loh, K. P. One-Pot Synthesis of Fluorescent Carbon Nanoribbons, Nanoparticles, and Graphene by the Exfoliation of Graphite in Ionic Liquids. *ACS Nano* **2009,** *3*, 2367–2375.
45. Liu, N.; Luo, F.; Wu, H.; Liu, Y.; Zhang, C.; Chen, J. One-Step Ionic-Liquid-Assisted Electrochemical Synthesis of Ionic-Liquid-Functionalized Graphene Sheets Directly from Graphite. *Adv. Funct. Mater.* **2008,** *18*, 1518–1525.
46. Kang, F.; Leng, Y.; Zhang, T. Y. Influences of H_2O_2 on Synthesis of H_2SO_4-GICs. *J. Phys. Chem. Solids* **1996,** *57*, 889–892.
47. Greinke, R. A.; Reyolds, R. A. Expandable Graphite and Method. U.S. Patent 6416815 B2, 2002.
48. Varchon, F; Mallet, P; Magaud, L; Veuillen, J. Y. Rotational Disorder in Few-Layer Graphene Films on 6H-SiC(000−1): A Scanning Tunneling Microscopy Study. *Phys. Rev. B* **2008,** *77*, 165415.
49. Guo, X.; Xiao, H. S.; Wang, F.; Zhang, Y. H. Micro-Raman and FTIR Spectroscopic Observation on the Phase Transitions of $MnSO_4$ Droplets and Ionic Interactions between Mn^{2+} and SO_4^{2-}. *J. Phys. Chem. A* **2010,** *114*, 6480–6486.
50. Krauss, B.; Lohmann, T.; Chae, D. H.; Haluska, M.; von Klitzing, K.; Smet, J. H. Laser-Induced Disassembly of a Graphene Single Crystal into a Nanocrystalline Network. *Phys. Rev. B* **2009,** *79*, 165428–9.
51. Gupta, A; Chen, G; Joshi, P.; Tadigadapa, S; Eklund, P. C. Raman Scattering from High-Frequency Phonons in Supported *n*-Graphene Layer Films. *Nano Lett.* **2006,** *6*, 2667–2673.
52. Graf, D.; Molitor, F.; Ensslin, K.; Stampfer, C.; Jungen, A.; Hierold, C.; Wirtz, L. Spatially Resolved Raman Spectroscopy of Single- and Few-Layer Graphene. *Nano Lett.* **2007,** *7*, 238–242.
53. Ferrari, A. C.; Meyer, J. C.; Scardaci, V.; Casiraghi, C.; Lazzeri, M.; Mauri, F.; Piscanec, S.; Jiang, D.; Novoselov, K. S.; Roth, S.; *et al.*Raman Spectrum of Graphene and Graphene Layers. *Phys. Rev. Lett.* **2006,** *97*, 187401.
54. Ni, Z. H.; Wang, H. M.; Kasim, J.; Fan, H. M.; Yu, T.; Wu, Y. H.; Feng, Y. P.; Shen, Z. X. Graphene Thickness Determination

Using Reflection and Contrast Spectroscopy. *Nano Lett.* **2007,** *7*, 2758–2763.
55. Lee, C. W.; Weng, C. H.; Wei, L.; Chen, Y.; Chan, M. B.; Tsai, C. H.; Leou, K. C.; Poa, C. H.; Wang, J.; Li, L J. Toward High-Performance Solution-Processed Carbon Nanotube Network Transistors by Removing Nanotube Bundles. *J. Phys. Chem. C* **2008,** *112*, 12089–12091.
56. Zhang, W.; Li, L. J. The Screening of Charged Impurities in Bilayer Graphene. *New J. Phys.* **2010,** *12*, 103037.